8 Architectures for reference-based and blind multilayer detection

Karl-Dirk Kammeyer, Jürgen Rinas, and Dirk Wübben

Multilayer systems are predestinated for high-rate wireless data transmission, where the source simultaneously radiates several data streams via multiple transmit antennas. The main computational effort of transmission schemes of this type is required at the receiver for separating the superimposed information signals. We distinguish between two types of detection schemes, where the first type requires channel knowledge for the receiver and the second type performs a totally blind data estimation.

Recently, several detection algorithms have been investigated under the assumption of known channel state information at the receiver. This channel knowledge may be obtained by pilot-aided transmission and channel estimation. For these reference-aided transmission the well-known linear detection schemes are generally outperformed by successive detection schemes, namely, the V-BLAST algorithm. In order to decrease the required computational complexity of this nonlinear scheme, we will restate it by applying the QR decomposition of the channel matrix. This yields the same successive interference cancelation (SIC) detection algorithm with complexity comparable to linear detection.

A detection approach avoiding pilot symbols is given by the concept of blind source separation (BSS). BBS approaches normally lead to linear spatial filters. In order to achieve the performance of reference-based detection, an iterative combination of BSS and nonlinear SIC is proposed. Furthermore, the application of BSS is favorable in many practical cases, as the sophisticated MIMO estimation problems can be transformed to well-known solutions for SISO communication.

The performances of the discussed schemes are demonstrated by simulations as well as by measurement results.

8.1. System model

Within this chapter, we consider the single-user multiple-antenna system in Figure 8.1 with N_T transmit and $N_R \geq N_T$ receive antennas in a non-frequency-selective environment. At the transmitter, the binary information data is demultiplexed into N_T data substreams of equal length and mapped onto PSK or QAM symbols of

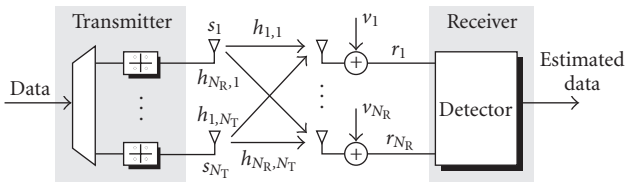

FIGURE 8.1. Model of a MIMO system with N_T transmit and N_R receive antennas.

the alphabet $\mathcal{A}$ with cardinality $|\mathcal{A}|$. These substreams are organized in frames of length M and simultaneously transmitted over the N_T antennas. Thus, the investigated scheme corresponds to the V-BLAST (vertical Bell Labs layered space-time) architecture introduced in [1, 2].

In order to describe the MIMO system, the discrete-time complex baseband model is investigated. Let $s_p[m]$ denote the symbol transmitted at time instant $1 \le m \le M$ from antenna $1 \le p \le N_T$. By defining the $N_T \times 1$ transmit signal vector $\mathbf{s}[m] = [s_1[m] \cdots s_{N_T}[m]]^T$ the corresponding $N_R \times 1$ receive signal vector $\mathbf{r}[m] = [r_1[m] \cdots r_{N_R}[m]]^T$ is given by

$$\mathbf{r}[m] = \mathbf{H}\mathbf{s}[m] + \mathbf{v}[m]. \tag{8.1}$$

In (8.1), $\mathbf{v}[m] = [v_1[m] \cdots v_{N_R}[m]]^T$ represents white Gaussian noise of variance σ_v^2 observed at the N_R receive antennas while the average transmit power of each antenna is normalized to one, that is,[1] $\mathrm{E}\{\mathbf{s}[m]\mathbf{s}^H[m']\} = \mathbf{I}_{N_T}\delta(m-m')$ and $\mathrm{E}\{\mathbf{v}[m]\mathbf{v}^H[m']\} = \sigma_v^2\mathbf{I}_{N_R}\delta(m-m')$. The $N_R \times N_T$ channel matrix $\mathbf{H} = [\mathbf{h}_1, \ldots, \mathbf{h}_{N_T}]$ with column vectors $\mathbf{h}_p$ contains uncorrelated complex Gaussian fading gains $h_{k,p}$ with unit variance. We assume that the channel matrix $\mathbf{H}$ is constant over a frame of length M and changes independently from one frame to another (*block fading channel*). As the time slots m in (8.1) are independent of each other, we will drop the time index m in the sequel resulting in

$$\mathbf{r} = \mathbf{H}\mathbf{s} + \mathbf{v}. \tag{8.2}$$

In order to investigate the maximum performance achievable, we introduce the singular value decomposition (SVD) $\mathbf{H} = \mathbf{U}\mathbf{\Sigma}\mathbf{V}^H$ of the channel matrix $\mathbf{H}$, where $\mathbf{U}$ and $\mathbf{V}$ are unitary matrices and the diagonal matrix $\mathbf{\Sigma} = \mathrm{diag}[\sigma_1, \ldots, \sigma_{N_T}]$ contains the singular values $\sigma_p \ge 0$ [3]. By calculating the filtered receive vector

$$\mathbf{r}' = \mathbf{U}^H\mathbf{r} = \mathbf{\Sigma}\underbrace{\mathbf{V}^H\mathbf{s}}_{\mathbf{s}'} + \underbrace{\mathbf{U}^H\mathbf{v}}_{\mathbf{v}'} = \mathbf{\Sigma}\mathbf{s}' + \mathbf{v}' \tag{8.3}$$

the MIMO system (8.2) is decomposed into N_T parallel single-input single-output

[1] δ defines the Kronecker delta with $\delta(0) = 1$ and $\delta(n) = 0$ for $n \ne 0$.

(SISO) systems

$$r'_p = \sigma_p s'_p + \nu'_p, \tag{8.4}$$

where s'_p denotes a modified transmit signal. Obviously, information can only be transmitted over those equivalent SISO channels with nonzero singular values σ_p. If the number of transmission layers exceeds the number of *strong* singular values, the performance degrades. This effect is demonstrated in Section 8.4 with respect to measurements.

Several schemes have been investigated to estimate the transmitted information at the receiver. One class of detection algorithms requires an estimate of the channel state information (CSI), whereas a second class applies higher-order statistics to separate the distinct transmit signals. In the sequel both detection principles are investigated and a hybrid scheme exploiting the advantages of each principle is proposed.

8.2. Reference-based detection algorithms

Within this section we discuss several detection schemes under the assumption of perfect channel state information at the receiver. Therefore, the achieved performances give the upper bound for the blind and non-blind schemes in the subsequent section.

8.2.1. Maximum-likelihood detection

In order to detect the transmitted information, it would be optimal to use a maximum-likelihood (ML) detector. For each time instant m this optimum ML detector searches over the whole set of transmit signals $\mathbf{s} \in \mathcal{A}^{N_T}$, and decides in favor of the transmit signal $\hat{\mathbf{s}}$ that minimizes the Euclidean distance to the receive vector $\mathbf{r}$, that is,

$$\hat{\mathbf{s}}_{\mathrm{ML}} = \arg \min_{\mathbf{s} \in \mathcal{A}^{N_T}} \|\mathbf{r} - \mathbf{H}\mathbf{s}\|^2. \tag{8.5}$$

As the computational effort for each time instant is of order $|\mathcal{A}|^{N_T}$, brute force ML detection is not feasible for larger number of transmit antennas or higher modulation schemes. As an example, for a system with $N_T = 4$ transmit antennas and 16-QAM modulation, the ML detection requires the computation of $16^4 = 65536$ Euclidean distances for each transmit vector.

A feasible alternative is the application of the sphere detector [4], which restricts the search space to a sphere around $\mathbf{r}$. However, the computational complexity is still high in comparison to simple but suboptimal linear detection or successive interference cancelation. In the sequel, we investigate these suboptimum linear and nonlinear schemes. The advantage of both strategies is that the computational overhead is only required once for each transmitted frame, so for a large frame

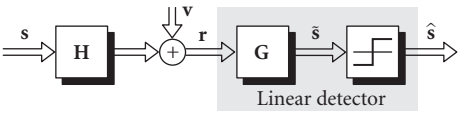

FIGURE 8.2. Block diagram of a MIMO scheme with linear detection.

length, the effort for each signal vector is very small. Furthermore, these suboptimum detection schemes may achieve near-ML performance in combination with lattice reduction, for example, see [5, 6].

8.2.2. Linear detection

The linear detector (LD) is the simplest approach for estimating the transmitted signals. The receive signal vector $\mathbf{r}$ is multiplied with a filter matrix $\mathbf{G}$, followed by a parallel decision on all layers, as shown in the block diagram in Figure 8.2.

In case of the zero-forcing (ZF) solution, the mutual interference between the layers is completely suppressed. This is accomplished by the Moore-Penrose pseudoinverse (denoted by $(\cdot)^+$) of the channel matrix

$$\mathbf{G}_{\mathrm{ZF}} = \mathbf{H}^+ = \left(\mathbf{H}^H\mathbf{H}\right)^{-1}\mathbf{H}^H, \tag{8.6}$$

where we assume that $\mathbf{H}$ has full column rank. The decision step consists of mapping each element of the filter output vector

$$\tilde{\mathbf{s}} = \mathbf{G}_{\mathrm{ZF}}\mathbf{r} = \mathbf{H}^+\mathbf{r} = \mathbf{s} + \left(\mathbf{H}^H\mathbf{H}\right)^{-1}\mathbf{H}^H\mathbf{v} \tag{8.7}$$

onto an element of the symbol alphabet $\mathcal{A}$ by an elementwise minimum distance quantization, that is, $\hat{s}_p = \mathcal{Q}_{\mathcal{A}}\{\tilde{s}_p\}$. The estimation errors of the different layers correspond to the main diagonal elements of the error covariance matrix

$$\mathbf{\Phi}_{ee,\mathrm{ZF}} = \mathrm{E}\{(\tilde{\mathbf{s}} - \mathbf{s})(\tilde{\mathbf{s}} - \mathbf{s})^H\} = \sigma_v^2\left(\mathbf{H}^H\mathbf{H}\right)^{-1}, \tag{8.8}$$

which equals the covariance matrix of the noise after the receive filter. It is obvious that small eigenvalues of $\mathbf{H}^H\mathbf{H}$ will lead to large errors due to noise amplification.

In order to improve the performance of the linear detector the noise term can be included in the design of the filter matrix $\mathbf{G}$. This is done by the minimum mean square error (MMSE) detector, where the filter

$$\mathbf{G}_{\mathrm{MMSE}} = \left(\mathbf{H}^H\mathbf{H} + \sigma_v^2\mathbf{I}_{N_{\mathrm{T}}}\right)^{-1}\mathbf{H}^H \tag{8.9}$$

represents a trade-off between noise amplification and interference suppression. The resulting filter output signal is given by

$$\tilde{\mathbf{s}} = \mathbf{G}_{\mathrm{MMSE}}\mathbf{r} = \left(\mathbf{H}^H\mathbf{H} + \sigma_v^2\mathbf{I}_{N_{\mathrm{T}}}\right)^{-1}\mathbf{H}^H\mathbf{r} \tag{8.10}$$

and the error covariance matrix is found to be

$$\mathbf{\Phi}_{ee,\mathrm{MMSE}} = \sigma_v^2 \left(\mathbf{H}^H \mathbf{H} + \sigma_v^2 \mathbf{I}_{N_\mathrm{T}}\right)^{-1}. \tag{8.11}$$

For the derivation of the nonlinear MMSE detection algorithm considered later it will be useful to point out the correspondence of the MMSE and the ZF criterion. To this end, we define an $(N_\mathrm{T} + N_\mathrm{R}) \times N_\mathrm{T}$ *extended* channel matrix[2] $\underline{\mathbf{H}}$ and an $(N_\mathrm{T} + N_\mathrm{R}) \times 1$ *extended* receive vector $\underline{\mathbf{r}}$ through [7, 8]

$$\underline{\mathbf{H}} = \begin{bmatrix} \mathbf{H} \\ \sigma_v \mathbf{I}_{N_\mathrm{T}} \end{bmatrix}, \qquad \underline{\mathbf{r}} = \begin{bmatrix} \mathbf{r} \\ \mathbf{0}_{N_\mathrm{T},1} \end{bmatrix}. \tag{8.12}$$

With these definitions we can rewrite the output of the MMSE filter (8.10) as

$$\tilde{\mathbf{s}} = \left(\begin{bmatrix} \mathbf{H}^H \sigma_v \mathbf{I}_{N_\mathrm{T}} \end{bmatrix} \begin{bmatrix} \mathbf{H} \\ \sigma_v \mathbf{I}_{N_\mathrm{T}} \end{bmatrix} \right)^{-1} \begin{bmatrix} \mathbf{H}^H \sigma_v \mathbf{I}_{N_\mathrm{T}} \end{bmatrix} \begin{bmatrix} \mathbf{r} \\ \mathbf{0}_{N_\mathrm{T},1} \end{bmatrix} \tag{8.13}$$

$$= \left(\underline{\mathbf{H}}^H \underline{\mathbf{H}}\right)^{-1} \underline{\mathbf{H}}^H \underline{\mathbf{r}} = \underline{\mathbf{H}}^{+} \underline{\mathbf{r}}. \tag{8.14}$$

Furthermore, the error covariance matrix (8.11) becomes

$$\mathbf{\Phi}_{ee,\mathrm{MMSE}} = \sigma_v^2 \left(\underline{\mathbf{H}}^H \underline{\mathbf{H}}\right)^{-1}. \tag{8.15}$$

Comparing (8.14) and (8.15) to the corresponding expression for the linear zero-forcing detector in (8.7) and (8.8), the only difference is that the channel matrix $\mathbf{H}$ has been replaced by $\underline{\mathbf{H}}$. Thus, an MMSE detector can be interpreted as a ZF detector with respect to the extended system model. This simple observation will be important for incorporating the MMSE criterion into the nonlinear detection algorithm in the sequel.

8.2.3. Successive interference cancelation detection

Instead of detecting the transmitted symbols in parallel, the nonlinear successive interference cancelation (SIC) schemes detect the signals one after another. Similar to a decision-feedback equalizer, the estimated interference of already detected signals is subtracted from the receive signal $\mathbf{r}$ before detecting the remaining signals. Due to the effect of error propagation, the sequence of detecting the layers has a strong impact on the overall error performance [2].

V-BLAST algorithm. The original V-BLAST detection algorithm [2] is based on the linear zero-forcing solution (8.6), but detects the signals one after another and not in parallel. In order to achieve the best performance, it is optimal to choose always the layer with the largest *postdetection* signal-to-noise ratio (SNR), or equivalently with the smallest estimation error [2]. By rewriting the error covariance (8.8) as $\mathbf{\Phi}_{ee,\mathrm{ZF}} = \sigma_v^2 \mathbf{G}_\mathrm{ZF} \mathbf{G}_\mathrm{ZF}^H$, the pth diagonal element corresponds to $\sigma_v^2 \mathbf{g}_{(p)} \mathbf{g}_{(p)}^H$,

[2]Henceforth, *underlined* variables indicate the application of this *extended* MMSE system model.

with $\mathbf{g}_{(p)}$ denoting row p of $\mathbf{G}_{\mathrm{ZF}}$. Consequently, the smallest estimation error corresponds to the row of $\mathbf{G}_{\mathrm{ZF}}$ with minimum Euclidean norm. Assuming that row i has the smallest norm in the first detection step, the corresponding filter output signal is given by

$$\tilde{s}_i = \mathbf{g}_{(i)}\mathbf{r} = s_i + \mathbf{g}_{(i)}\mathbf{v} \tag{8.16}$$

and the estimated signal $\hat{s}_i = \mathcal{Q}_{\mathcal{A}}\{\tilde{s}_i\}$ is found by quantization. The estimated interference caused by this signal is then subtracted from the receive signal vector $\mathbf{r}$ and the ith column is removed from the channel matrix, leading to a system with only $N_{\mathrm{T}} - 1$ transmit antennas. This procedure of nulling and canceling is repeated for the reduced systems until all signals are detected.

The adaptation to the MMSE criterion was presented in several publications (e.g., [9]), where the optimal detection sequence maximizes the signal-to-interference-and-noise ratio (SINR) in each decision step. Again, this corresponds to choosing the layer with the smallest estimation error in (8.11) or (8.15). Using similar arguments as before, the layer with highest SINR corresponds to the row of $\underline{\mathbf{H}}^{+}$ with minimum norm. It is worth to note that this best layer is not necessarily associated with the row of $\mathbf{G}_{\mathrm{MMSE}}$ with minimum norm, as $\mathbf{G}_{\mathrm{MMSE}}$ is not a square root of $\mathbf{\Phi}_{ee,\mathrm{MMSE}}$ [10]. Consequently, a detector applying the ZF sorting criterion based on the Euclidean row norm of $\mathbf{G}_{\mathrm{MMSE}}$ in the MMSE case will lead to a significant performance loss.

The main drawback of the V-BLAST detection algorithm lies in the computational complexity, as it requires multiple calculations of the pseudoinverse of the channel matrix in the ZF case [11] or of the extended channel matrix in the MMSE case. Thus, several schemes with reduced complexity have been proposed, for example, [8, 12, 13, 14].

Within this section, we consider the scheme presented in [14] and extended in [8]. To this end, we restate the successive interference cancelation scheme using the QR decomposition of the channel matrix, for the ZF as well as the MMSE case. In order to efficiently achieve an optimized detection order, we will then introduce a suboptimum approach, the so-called sorted QR decomposition. Later on, we extend this simple scheme by the postsorting algorithm, yielding the perfect detection sequence and thereby the performance of the V-BLAST scheme. The main advantage of this combined scheme comes with the complexity reduction, as it only requires a fraction of the computational effort of the original V-BLAST algorithm [8, 11].

ZF-SIC with QR decomposition. It was shown in several publications, for example, [11, 14, 15, 16, 17], that the zero-forcing solution of the V-BLAST algorithm can be restated in terms of the QR decomposition of the channel matrix $\mathbf{H} = \mathbf{QR}$, where the $N_{\mathrm{R}} \times N_{\mathrm{T}}$ matrix $\mathbf{Q}$ has unitary columns and the $N_{\mathrm{T}} \times N_{\mathrm{T}}$ matrix $\mathbf{R} = (r_{i,j})_{1\le i,j\le N_{\mathrm{T}}}$ is upper triangular [3]. Multiplying the receive signal $\mathbf{r}$ with $\mathbf{Q}^{H}$ yields the sufficient statistic

$$\tilde{\mathbf{s}} = \mathbf{Q}^{H}\mathbf{r} = \mathbf{R}\mathbf{s} + \tilde{\mathbf{v}} \tag{8.17}$$

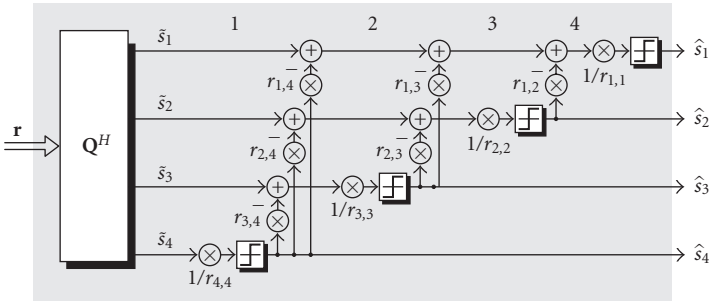

FIGURE 8.3. Block diagram of the successive interference cancelation detector for a system with $N_T = 4$ transmit antennas.

for the estimation of transmit vector $\mathbf{s}$. As $\mathbf{Q}$ is a unitary matrix, the statistical properties of the Gaussian noise term $\tilde{\mathbf{v}} = \mathbf{Q}^H\mathbf{v}$ remain unchanged and in a componentwise notation (8.17) becomes

$$\begin{bmatrix} \tilde{s}_1 \\ \tilde{s}_2 \\ \vdots \\ \tilde{s}_{N_T} \end{bmatrix} = \begin{bmatrix} r_{1,1} & r_{1,2} & \cdots & r_{1,N_T} \\ \vdots & r_{2,2} & & \vdots \\ \vdots & & \ddots & \vdots \\ \mathbf{0} & \cdots & & r_{N_T,N_T} \end{bmatrix} \begin{bmatrix} s_1 \\ s_2 \\ \vdots \\ s_{N_T} \end{bmatrix} + \begin{bmatrix} \tilde{v}_1 \\ \tilde{v}_2 \\ \vdots \\ \tilde{v}_{N_T} \end{bmatrix}. \tag{8.18}$$

Due to the upper triangular structure of $\mathbf{R}$, the pth element of $\tilde{\mathbf{s}}$ is given by

$$\tilde{s}_p = r_{p,p}s_p + \sum_{i=p+1}^{N_T} r_{p,i}s_i + \tilde{v}_p \tag{8.19}$$

and is free of interference from layers $1, \ldots, p-1$. Thus, $\tilde{s}_{N_T}$ is totally free of interference and can be used to estimate s_{N_T} after appropriate scaling with $1/r_{N_T,N_T}$. Proceeding with $\tilde{s}_{N_T-1}, \ldots, \tilde{s}_1$ and assuming correct previous decisions, the interference can be perfectly canceled in each step. Then it follows from (8.19) that the SNR of layer p is determined by the diagonal element $|r_{p,p}|^2$. For a system with $N_T = 4$ transmit antennas the successive detection and cancelation procedure is shown in Figure 8.3.

The signal spaces of the corresponding detection and interference cancelation steps are shown in Figure 8.4 (achieved with the experimental equipment described in Section 8.4). The first depicted column (step 1) corresponds to $\tilde{\mathbf{s}}$ (scaled by $r_{4,4}$ for illustration purpose), the output of the filter matrix $\mathbf{Q}^H$. Obviously layer 4 is free of interference and can be estimated, whereas the other layers are still affected by interference. The second column shows the signal space after subtracting the estimated interference, that is, step 2 in Figure 8.3. Thus, layer 3 may be detected. The succeeding steps are straightforward.

MMSE-SIC with QR decomposition. In order to extend the QR-based detection with respect to the MMSE criterion, we can exploit the similarity of linear ZF and

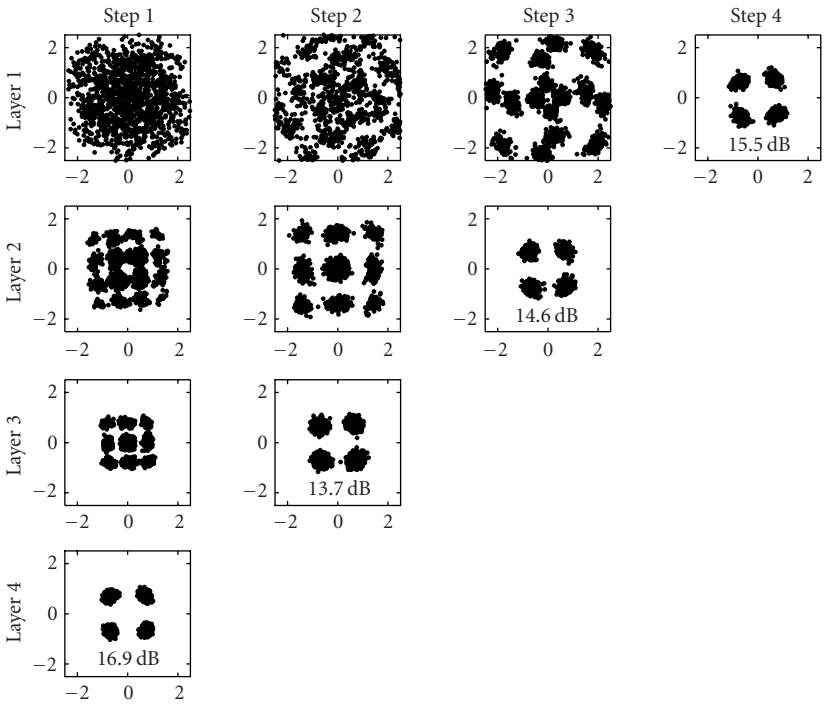

FIGURE 8.4. Signal space of each layer at the distinct steps of the successive interference cancelation for a system with $N_T = 4$ transmit antennas, $N_R = 4$ receive antennas and QPSK modulation with estimated SNR.

MMSE detection. For this purpose, we introduce the QR decomposition of the extended channel matrix (8.12)

$$\underline{\mathbf{H}} = \begin{bmatrix} \mathbf{H} \\ \sigma_v \mathbf{I}_{N_T} \end{bmatrix} = \underline{\mathbf{Q}}\underline{\mathbf{R}} = \begin{bmatrix} \mathbf{Q}_1 \\ \mathbf{Q}_2 \end{bmatrix} \underline{\mathbf{R}} = \begin{bmatrix} \mathbf{Q}_1\underline{\mathbf{R}} \\ \mathbf{Q}_2\underline{\mathbf{R}} \end{bmatrix}, \tag{8.20}$$

where the unitary $(N_T+N_R)\times N_T$ matrix $\underline{\mathbf{Q}}$ was partitioned into the $N_R \times N_T$ matrix $\mathbf{Q}_1$ and the $N_T \times N_T$ matrix $\mathbf{Q}_2$ and $\underline{\mathbf{R}} = (\underline{r}_{i,j})_{1\le i,j\le N_T}$ denotes the corresponding upper triangular matrix. Obviously,

$$\underline{\mathbf{Q}}^H\underline{\mathbf{H}} = \mathbf{Q}_1^H\mathbf{H} + \sigma_v\mathbf{Q}_2^H = \underline{\mathbf{R}} \tag{8.21}$$

holds and from the relation $\sigma_v\mathbf{I}_{N_T} = \mathbf{Q}_2\underline{\mathbf{R}}$ in (8.20), it follows that

$$\underline{\mathbf{R}}^{-1} = \frac{1}{\sigma_v}\mathbf{Q}_2, \tag{8.22}$$

that is, the inverse $\underline{\mathbf{R}}^{-1}$ is a by-product of the QR decomposition and $\mathbf{Q}_2$ is an upper triangular matrix. This relation will be useful for the postsorting algorithm

proposed later on. Using (8.21), the filtered receive vector becomes

$$\tilde{\mathbf{s}} = \underline{\mathbf{Q}}^H \underline{\mathbf{r}} = \mathbf{Q}_1^H \mathbf{r} = \underline{\mathbf{R}}\mathbf{s} - \sigma_v \mathbf{Q}_2^H \mathbf{s} + \mathbf{Q}_1^H \mathbf{v}. \tag{8.23}$$

The second term on the right-hand side of (8.23) including the lower triangular matrix $\mathbf{Q}_2^H$ constitutes the remaining interference that cannot be removed by the successive interference cancelation procedure. This points out the trade-off between noise amplification and interference suppression.

As mentioned in the discussion of the V-BLAST algorithm, the order of detection is crucial due to error propagation. Within the QR-based SIC the detection order can be changed by permuting the columns of $\underline{\mathbf{H}}$ and the corresponding elements in $\mathbf{s}$. The optimum detection sequence now maximizes the signal-to-interference-and-noise ratio (SINR) for each layer, leading to a minimum estimation error for the corresponding detection step. The estimation errors of the different layers in the first detection step correspond to the diagonal elements of the error covariance matrix (8.15)

$$\mathbf{\Phi}_{ee,\mathrm{MMSE}} = \sigma_v^2 \left(\underline{\mathbf{H}}^H \underline{\mathbf{H}}\right)^{-1} = \sigma_v^2 \underline{\mathbf{R}}^{-1} \underline{\mathbf{R}}^{-H}. \tag{8.24}$$

The estimation error for layer p after perfect interference cancelation is given by $\sigma_v^2/|\underline{r}_{p,p}|^2$. Thus, it is optimal to choose the permutation of $\underline{\mathbf{H}}$ that maximizes $|\underline{r}_{p,p}|$ in each detection step, that is, in the order $N_\mathrm{T}, \ldots, 1$. The algorithm proposed in the next paragraph determines an improved detection sequence within a single *sorted* QR decomposition and thereby significantly reduces the computational complexity in comparison to the V-BLAST algorithm.

Sorted QR decomposition (SQRD). In order to obtain the optimal detection order, first $|\underline{r}_{N_\mathrm{T},N_\mathrm{T}}|$ has to be maximized over all possible permutations of the columns of the extended channel matrix $\underline{\mathbf{H}}$, followed by $|\underline{r}_{N_\mathrm{T}-1,N_\mathrm{T}-1}|$, and so on. Unfortunately, using standard algorithms for the QR decomposition, the diagonal elements of $\underline{\mathbf{R}}$ are calculated just in the opposite order, starting with $\underline{r}_{1,1}$. This makes finding the optimal order of detection a difficult task.

A heuristic approach of arranging the order of detection within the QR decomposition for the ZF detection was presented in [11, 14] and extended to the MMSE criterion in [8, 16]. This sorted QR decomposition algorithm is basically an extension to the modified Gram-Schmidt procedure by reordering the columns of the channel matrix prior to each orthogonalization step. The fundamental idea is based on the fact that the determinant of the Gram matrix $\underline{\mathbf{H}}^H \underline{\mathbf{H}}$, that is, the squared volume of the parallelepiped spanned by $\underline{\mathbf{H}}$, is invariant to column exchanges [3]. Since this determinant can be rewritten as

$$\det\left(\underline{\mathbf{H}}^H \underline{\mathbf{H}}\right) = \det\left(\underline{\mathbf{R}}^H \underline{\mathbf{R}}\right) = \prod_{p=1}^{N_\mathrm{T}} \left|\underline{r}_{p,p}\right|^2 = \mathrm{const}, \tag{8.25}$$

the product $\underline{r}_{1,1} \cdot \ldots \cdot \underline{r}_{N_\mathrm{T},N_\mathrm{T}}$ is also independent of the chosen column order. Thus, the basic idea is to exchange the columns to *minimize* the diagonal elements $\underline{r}_{p,p}$

(1) $\underline{\mathbf{R}} = \mathbf{0}, \underline{\mathbf{Q}} = \underline{\mathbf{H}}, \mathbf{p} = [1 \cdots N_{\mathrm{T}}]$
(2) for $i = 1, \ldots, N_{\mathrm{T}}$
(3) $\quad \mathbf{norm}(i) = \|\underline{\mathbf{Q}}(:, i)\|^2$
(4) end
(5) for $i = 1, \ldots, N_{\mathrm{T}}$
(6) $\quad k_i = \arg\min \mathbf{norm}(i, \ldots, N_{\mathrm{T}})$
(7) $\quad$ exchange columns i and k_i in $\underline{\mathbf{R}}$, $\mathbf{p}$, $\mathbf{norm}$ and in the first $N_{\mathrm{R}} + i - 1$ rows of $\underline{\mathbf{Q}}$
(8) $\quad \underline{\mathbf{R}}(i, i) = \sqrt{\mathbf{norm}(i)}$
(9) $\quad \underline{\mathbf{Q}}(:, i) = \underline{\mathbf{Q}}(:, i)/\underline{\mathbf{R}}(i, i)$
(10) $\quad$ for $k = i + 1, \ldots, N_{\mathrm{T}}$
(11) $\quad\quad \underline{\mathbf{R}}(i, k) = \underline{\mathbf{Q}}(:, i)^H \underline{\mathbf{Q}}(:, k)$
(12) $\quad\quad \underline{\mathbf{Q}}(:, k) := \underline{\mathbf{Q}}(:, k) - \underline{\mathbf{R}}(i, k)\underline{\mathbf{Q}}(:, i)$
(13) $\quad\quad \mathbf{norm}(k) := \mathbf{norm}(k) - \underline{\mathbf{R}}(i, k)^2$
(14) $\quad$ end
(15) end

Algorithm 8.1. Pseudocode of MMSE-SQRD-algorithm.

in the order of their calculation, that is, in the sequence $\underline{r}_{1,1}, \ldots, \underline{r}_{N_{\mathrm{T}}, N_{\mathrm{T}}}$. As the product is constant, small $\underline{r}_{p,p}$ in the upper left part should lead to large elements in the lower right part of $\underline{\mathbf{R}}$.

Now, $\underline{r}_{1,1}$ is simply the norm of the column vector $\underline{\mathbf{h}}_1$, so the first optimization in the SQRD algorithm consists merely of permuting the column of $\underline{\mathbf{H}}$ with minimum norm to this position. During the following orthogonalization of the vectors $\underline{\mathbf{h}}_2, \ldots, \underline{\mathbf{h}}_{N_{\mathrm{T}}}$ with respect to the normalized vector $\underline{\mathbf{h}}_1$, the first row of $\underline{\mathbf{R}}$ is obtained. Next, $\underline{r}_{2,2}$ is determined in a similar fashion from the remaining $N_{\mathrm{T}} - 1$ orthogonalized vectors, and so forth. Thus, the extended channel matrix $\underline{\mathbf{H}}$ is successively transformed into the matrix $\underline{\mathbf{Q}}$ associated with the desired ordering, while the corresponding $\underline{\mathbf{R}}$ is calculated row by row. Note that the column norms have to be calculated only once in the beginning and can be easily updated afterwards. Hence, the computational overhead due to sorting is negligible. An in-place description of the whole MMSE-SQRD algorithm is given in[3] Algorithm 8.1, with vector $\mathbf{p}$ denoting the permutation of the columns of $\mathbf{H}$.

The reordering steps (lines (6) and (7) within the algorithm) require only a very small computational overhead compared to an unsorted QR decomposition [8]. However, the SQRD ordering strategy does not always lead to the perfect detection sequence, but in many cases of interest the performance degradation is small compared to the reduced complexity. Furthermore, whenever SQRD fails to find the optimal order, the postsorting algorithm described in the sequel assures the optimal sorting and thereby achieves the same performance as V-BLAST.

[3] $\mathbf{A}(a : b, c : d)$ denotes the submatrix of $\mathbf{A}$ with elements from rows $a, \ldots, b$ and columns $c, \ldots, d$.

Postsorting algorithm (PSA). In this section we briefly present the postsorting algorithm (PSA) introduced in [8]. In order to motivate the PSA, the structure of the error covariance matrix in case of optimal sorting is investigated in more detail. Due to the relation $\mathbf{Q}_2 = \sigma_v \underline{\mathbf{R}}^{-1}$ introduced in (8.22) the error covariance matrix (8.24) is given by

$$\mathbf{\Phi}_{ee,\mathrm{MMSE}} = \mathbf{Q}_2 \mathbf{Q}_2^H, \tag{8.26}$$

that is, $\mathbf{Q}_2$ is a square root of $\mathbf{\Phi}_{ee,\mathrm{MMSE}}$ [7]. Thus, the pth diagonal element of $\mathbf{\Phi}_{ee,\mathrm{MMSE}}$ is proportional to the norm of the pth row of $\mathbf{Q}_2$. Recalling the optimal ordering criterion, the last row of $\mathbf{Q}_2$ must have minimum norm of all rows. Assume that this condition is fulfiled, then the last row of the upper left $N_\mathrm{T}-1 \times N_\mathrm{T}-1$ submatrix of $\mathbf{Q}_2$ must have minimum norm of all rows of this submatrix. In case of the correct sorting this condition is accomplished by all upper left submatrices.

Now assume that this condition is not fulfiled for the matrix $\mathbf{Q}_2$. Then the row with minimum norm and the last row (as well as the corresponding elements of $\mathbf{p}$) need to be exchanged at the expense of destroying the upper triangular structure. However, by right multiplying the permuted version of $\mathbf{Q}_2$ with a proper unitary $N_\mathrm{T} \times N_\mathrm{T}$ Householder reflection matrix[4] $\mathbf{\Theta}$, a block triangular matrix is achieved. Finally, $\mathbf{Q}_1$ has to be updated to $\mathbf{Q}_1\mathbf{\Theta}$. Instead of permuting columns of $\underline{\mathbf{R}}$ and left multiplying with $\mathbf{\Theta}^H$ in each step, we can alternatively invert $\mathbf{Q}_2$ at the end of the PSA, due to the relation $\underline{\mathbf{R}} = 1/\sigma_v \mathbf{Q}_2^{-1}$. These ordering and reflection steps are then iterated for the upper left $(N_\mathrm{T} - 1) \times (N_\mathrm{T} - 1)$ submatrix of the such modified matrix $\mathbf{Q}_2$ and the first $N_\mathrm{T} - 1$ columns of the new matrix $\mathbf{Q}_1$, resulting in the QR decomposition of the optimally ordered channel matrix $\underline{\mathbf{H}}$. The whole postsorting algorithm is given in Algorithm 8.2.

Thus, a two-step decomposition and reordering procedure is achieved. This scheme finds the optimum detection sequence in the sense of V-BLAST and therefore leads to the same performance. However, the computational complexity of the whole detection process reduces to a fraction of the V-BLAST complexity and is comparable to the effort of linear detection [8].

Performance evaluation. In order to compare the different detection schemes we investigate the achieved bit error rates (BER) for a system with $N_\mathrm{T} = 4$, $N_\mathrm{R} = 4$, and QPSK modulation. E_b denotes the average energy per information bit arriving at the receiver, thus $E_b/N_0 = N_\mathrm{R}/(\log_2(|\mathcal{A}|)\sigma_v^2)$ holds. (Due to this normalization the antenna gain is canceled out.)

Figure 8.5a shows the performance of various ZF detection algorithms and the BER of ML detection. As expected, the successive detection algorithms outperform the linear ZF detector. The impact of an optimized detection order becomes

[4]The Householder matrix for a $1 \times n$ *row* vector $\mathbf{a}$ with complex elements is given by $\mathbf{\Theta} = \mathbf{I}_n - (1 + \xi)\mathbf{u}^H\mathbf{u}$ with the definitions $\mathbf{u} = (\mathbf{a} - \|\mathbf{a}\|\mathbf{e}_n)/\|\mathbf{a} - \|\mathbf{a}\|\mathbf{e}_n\|$, $\mathbf{e}_n = [\mathbf{0}_{1,n-1}1]$ and $\xi = \mathbf{u}\mathbf{a}^H/\mathbf{a}\mathbf{u}^H$. The multiplication of $\mathbf{a}$ with $\mathbf{\Theta}$ results in a vector consisting of $n - 1$ zero elements and one element equal to the norm of $\mathbf{a}$, that is, $\mathbf{a}\mathbf{\Theta} = [\mathbf{0}_{1,n-1}\|\mathbf{a}\|]$ holds.

(1) $k_{\min} = N_T$
(2) for $i = N_T, \ldots, 2$
(3) for $\ell = 1, \ldots, i$
(4) $\mathbf{error}(\ell) = \|\mathbf{Q}_2(\ell, 1 : i)\|^2$
(5) end
(6) $k_i = \arg\min \mathbf{error}(1, \ldots, i)$
(7) $k_{\min} := \min(k_{\min}, k_i)$
(8) if $k_i < i$
(9) exchange rows i and k_i in $\mathbf{Q}_2$
and columns i and k_i in $\mathbf{p}$
(10) end
(11) if $k_{\min} < i$
(12) calculate $\mathbf{\Theta}$ such that elements
of $\mathbf{Q}_2(i, k_{\min} : i - 1)$ become zero
(13) $\mathbf{Q}_2(1 : i, k_{\min} : i) := \mathbf{Q}_2(1 : i, k_{\min} : i)\mathbf{\Theta}$
(14) $\mathbf{Q}_1(:, k_{\min} : i) := \mathbf{Q}_1(:, k_{\min} : i)\mathbf{\Theta}$
(15) end
(16) end
(17) $\underline{\mathbf{R}} = 1/\sigma_v \mathbf{Q}_2^{-1}$

Algorithm 8.2. Pseudocode of MMSE-PSA-algorithm.

obvious by comparing the unsorted SIC, SQRD-SIC, and SQRD-PSA-SIC (or equivalently V-BLAST). As SQRD-SIC does not always find the optimum detection order it results in a performance gap of about 1 dB for a BER of 10^{-3} compared to SQRD-PSA-SIC. However, this degradation reduces for an increasing number of receive antennas, for example, for a system with $N_R = 6$ the difference is only 0.5 dB for a BER of 10^{-5} [11].

For the same system, Figure 8.5b shows the performance of the MMSE detection schemes. Comparing these results with the ZF schemes, a remarkable performance improvement can be observed. Furthermore, the SQRD-SIC achieves the same performance as the optimally sorted SQRD-PSA-SIC up to $E_b/N_0 = 10$ dB. In many cases of interest, the SQRD approach would be the first choice for implementation due to the reduced complexity. However, the combination of SQRD and PSA yields optimum SIC performance with a minimum of computational complexity [8].

8.3. Blind source separation

Blind source separation (BSS) is a general problem in multisensor multiantenna systems and aims at separating data streams from a mixture of signals that stem from statistical independent sources. There are many applications for this problem ranging from audio processing to medical applications and communications. In

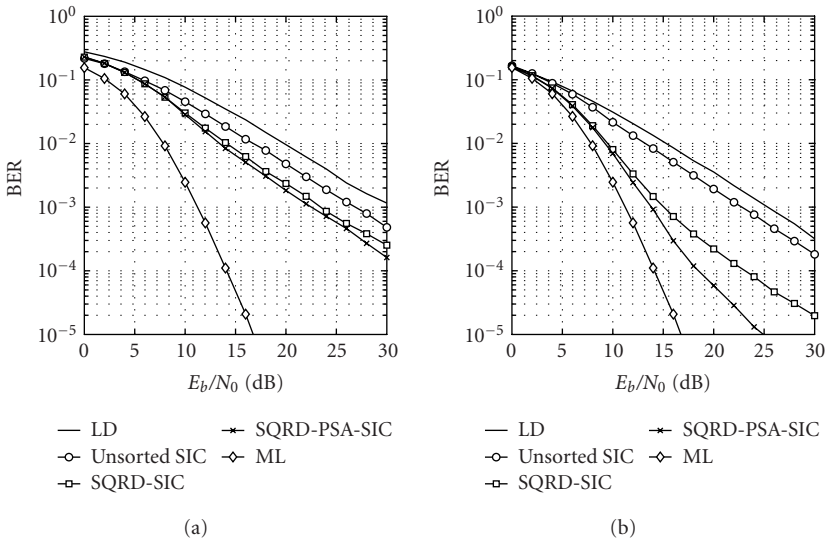

FIGURE 8.5. Bit error rate of (a) ZF and (b) MMSE detection of a system with $N_T = 4$ antennas and $N_R = 4$ antennas, uncoded QPSK symbols.

this section applications to current MIMO communication systems are presented. The investigated algorithms are termed blind, because the channel matrix $\mathbf{H}$ is not known and no additional pilot symbols are used to separate the data streams.

8.3.1. Linear separation

For the instantaneous (nonconvolutive) channel model

$$\mathbf{r} = \mathbf{H}\mathbf{s} + \mathbf{v} \tag{8.27}$$

of linear separation, the problem can be stated as follows. Blindly find a matrix $\mathbf{G}$ to be multiplied from the left-hand side onto $\mathbf{r}$ so that the statistically independent data streams $\mathbf{s}$ can be recovered. This leads to a linear detection of the data streams.

Possible approaches to this BSS problem. In general there are three types of information that can be utilized to solve the blind source separation problem [18]:

(i) *non-Gaussianity* of the source signals. This property is explicitly utilized in all higher-order statistics-(HOS-)based algorithms and will be explained later on in this text;

(ii) the different *coloring of the source signals*. This property can normally not be exploited in a communication context, because communication signals are designed to utilize a given bandwidth as good as possible and therefore the signals are mostly white. This type of information is used in the second order blind identification (SOBI) type of algorithms [19, 20];

(iii) *instationarity of the source signals* (or channel). This can be applied to audio and communication signals but requires fading or frequency-selective channels. This can also be utilized in SOBI-like approaches [19, 20].

The general idea of the HOS-based source separation algorithms will be described in this section in an illustrative way. We search for an $N_T \times N_R$ equalization matrix $\mathbf{G}$ that exploits the fact that the signal streams contained in the vector of the extracted signals

$$\mathbf{e} = \mathbf{G}\mathbf{r} \tag{8.28}$$

are statistically independent. The general definition of statistical independence is that the joint probability density function (pdf) is the product of the marginal densities[5]

$$p(e_1, e_2) = p(e_1) \cdot p(e_2). \tag{8.29}$$

In order to obtain simple algorithms from this abstract formulation, we need to apply some approximations. The simplest (first- and second-order) approach to this problem is to apply this multiplication property not to pdfs but to expectation values

$$\mathrm{E}\{e_1 \cdot e_2\} = \mathrm{E}\{e_1\} \cdot \mathrm{E}\{e_2\}. \tag{8.30}$$

Because in most practical cases communication signals have a mean value of zero, we can simplify this expression to

$$\mathrm{E}\{e_1 \cdot e_2\} = 0. \tag{8.31}$$

This can be interpreted as follows. The separation problem is split into two steps to determine the equalization matrix $\mathbf{G} = \mathbf{B}^H\mathbf{W}$. A first approximation towards a blind source separation is the decorrelation of the output signals with matrix $\mathbf{W}$. This computation step is also known as sphering, whitening, standardization, or principle component analysis. With the decorrelation the separation problem is not yet solved! The second step is to determine the unitary matrix $\mathbf{B}$. This can be accomplished using different algorithms and will be explained below.

The whitening matrix

$$\mathbf{W} = \mathbf{D}^{-1/2}\mathbf{U}^H \tag{8.32}$$

is calculated by taking the eigenvalue decomposition (EVD) $\mathbf{\Phi}_{rr} = \mathrm{E}\{\mathbf{r}\mathbf{r}^H\} = \mathbf{U}\mathbf{D}\mathbf{U}^H$ of the covariance of the received signals $\mathbf{r}$. Consequently, the decorrelated

[5] In this section we use a simplified notation, where we do not distinguish between random variables and their realizations.

signals can be obtained by

$$\mathbf{z} = \mathbf{W}\mathbf{r}, \quad \mathbf{\Phi}_{zz} = \mathrm{E}\{\mathbf{z}\mathbf{z}^H\} = \mathbf{I}_{N_\mathrm{T}}. \tag{8.33}$$

This procedure can be used in a similar way to limit $\mathbf{z}$ to the dominant subspace directions (corresponding to the greatest eigenvalues) in order to reduce the number of dimensions and the noise influence [21].

Since the decorrelation will lead to orthogonality but not statistical independence, we have to search for further degrees of freedom. One remaining degree of freedom is an $N_\mathrm{T} \times N_\mathrm{T}$ unitary matrix $\mathbf{B}$, if we do not want to destroy the spatial orthogonality of $\mathbf{z}$, that is,

$$\mathbf{I} \stackrel{!}{=} \mathrm{E}\{\mathbf{B}^H\mathbf{z}\mathbf{z}^H\mathbf{B}\} = \mathbf{B}^H\mathrm{E}\{\mathbf{z}\mathbf{z}^H\}\mathbf{B} = \mathbf{B}^H\mathbf{B}. \tag{8.34}$$

The basic criterion to determine $\mathbf{B}$ is the maximization of the kurtosis of a separated signal stream. The kurtosis is a fourth-order (auto-)cumulant

$$\mathrm{kurt}\{e\} = \mathrm{E}\{|e|^4\} - \mathrm{E}\{ee^*\}\mathrm{E}\{ee^*\} - \mathrm{E}\{ee\}\mathrm{E}\{e^*e^*\} - \mathrm{E}\{ee^*\}\mathrm{E}\{e^*e\} \tag{8.35}$$

that can be interpreted as a fourth-order moment minus the Gaussian parts of the distribution, so that its value is zero for Gaussian distributed signals. A mixture of many independent signals (as it is provided by the MIMO channel) will lead to a Gaussian distribution due to the central limit theorem of statistics. Therefore the non-Gaussianity in terms of the kurtosis is one possible criterion that is utilized in the two algorithms that are briefly explained below.[6]

JADE. The joint approximate diagonalization of eigenmatrices (JADE) algorithm [21] is one common batch procedure that solves the separation problem. The first step of this algorithm is to decorrelate the input streams as shown in (8.33). The final separation is done by additionally utilizing fourth-order information. Therefore, the JADE algorithm maximizes some elements of the cumulant matrix $\mathrm{cum}(e_i^\star, e_i, e_j^\star, e_l)$[7] obtained from the extracted signals $\mathbf{e}$ defined in (8.28)

$$\max_{\mathbf{B}} \sum_{i,j,l=1}^{N_\mathrm{T}} \left| \mathrm{cum}\left(e_i^\star, e_i, e_j^\star, e_l\right) \right|^2. \tag{8.36}$$

This optimization problem is solved by an eigenvalue decomposition of the cumulant matrix and a joint diagonalization of the dominant cumulant eigenvectors rearranged as matrices. This diagonalization is done by a Jacobi-like procedure

[6] Compared to this illustrative explanation of BSS algorithms more mathematical ones can be found in specialized textbooks [20, 22, 23] or in [24].

[7] $\mathrm{cum}(e_i^\star, e_i, e_j^\star, e_l)$ is a fourth-order cross-cumulant of the extracted signals e_p. Cumulants can be interpreted as higher-order moments minus their Gaussian parts of the distribution. For further details see [25].

using Givens rotations and leads to the unitary $N_T \times N_T$ matrix $\mathbf{B}$ and the independent data streams

$$\mathbf{e} = \underbrace{\mathbf{B}^H \mathbf{W}}_{\mathbf{G}} \mathbf{r} = \mathbf{B}^H \mathbf{z}. \tag{8.37}$$

For details see [21]. A similar approach that needs less computational effort is the SSARS algorithm presented in [26].

FastICA. The FastICA algorithm is organized in a different way [10, 27] compared with the JADE algorithm. The basic idea of this algorithm is to apply a blind source extraction (BSE) for each component separately and to prevent the same signal from being extracted multiple times. It starts with the whitening of the received data as presented in (8.33).

In order to extract signal number p out of the whitened mixture $\mathbf{z}$, a randomly initialized extraction vector $\mathbf{b}_p$—a column vector of the $N_T \times N_T$ matrix $\mathbf{B}$—is generated. In order to preserve the signals to remain uncorrelated, $\mathbf{B}$ has again to be a unitary matrix. Therefore, $\mathbf{b}_p$ is constrained to form an orthonormal basis using the knowledge of the vectors $\mathbf{b}_1 \cdots \mathbf{b}_{p-1}$ obtained in previous iterations. To reach this goal matrix,

$$\mathbf{B}_p = [\mathbf{b}_1, \mathbf{b}_2, \ldots, \mathbf{b}_p] \tag{8.38}$$

containing the extraction vectors of the former iterations is built. The randomly initialized vector $\mathbf{b}_p$ is orthogonalized with respect to the space spanned by $\mathbf{B}_{p-1}$

$$\mathbf{b}'_p = \mathbf{b}_p - \mathbf{B}_{p-1}\mathbf{B}^H_{p-1}\mathbf{b}_p \tag{8.39}$$

and normalized to a length of one

$$\mathbf{b}''_p = \frac{\mathbf{b}'_p}{||\mathbf{b}'_p||}. \tag{8.40}$$

In order to determine $\mathbf{b}_p$ we choose the maximization of the kurtosis of a single signal as the criterion

$$\max_{\mathbf{b}_p} J_{\text{FastICA},p}(e_p) = \max_{\mathbf{b}_p} \text{kurt}\left\{ |e_p|^4 \right\} = \max_{\mathbf{b}_p} \text{kurt}\left\{ |\mathbf{b}_p^H \mathbf{z}|^4 \right\}. \tag{8.41}$$

This can be solved using a fixed-point iteration including the additional constraints (8.39) and (8.40) [10]. The resulting signal streams $\mathbf{e}$ can be extracted by multiplying the received signal with the matrix of all collected extraction vectors $\mathbf{B} = \mathbf{B}_{N_T}$ according to (8.37).

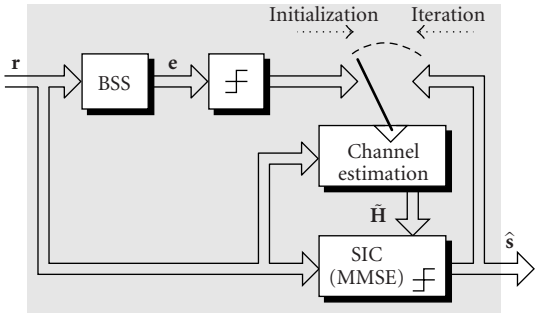

FIGURE 8.6. Block diagram of hybrid BSS detection.

Symbol decision. The algorithms presented in the previous sections only provide statistically independent data streams **e**. Therefore the signal streams can be rotated by an arbitrary phase factor—modeled by the diagonal matrix $\mathbf{\Psi} = \text{diag}\,[\psi_1, \ldots, \psi_{N_T}]$—and can be permuted by a matrix **P**. In general the permutation problem cannot be solved without additional addressing in the data streams or other side information, but the phase problem can be tackled by utilizing knowledge of the symbol alphabet. If QPSK is used as a modulation form, the phase can be estimated up to a discrete phase or quadrant ambiguity $\hat{\mathbf{\Psi}} = \text{diag}\,[\hat{\psi}_1, \ldots, \hat{\psi}_p, \ldots, \hat{\psi}_{N_T}]$, $\hat{\psi}_p \in \{0, \pi/2, \pi, (3/2)\pi\}$, which can be corrected by

$$e_{p,\text{derot}}[m] = e_p[m] \cdot e^{-j(1/4)\arg\{-\sum_{m'=1}^{M} e_p^4[m']\}} \quad \forall\, p \in 1, \ldots, N_T. \tag{8.42}$$

The remaining discrete ambiguity $\hat{\mathbf{\Psi}}$ can be removed by differential modulation forms or rotational invariant coding. But a decision of the pure symbols **s** is only possible with a remaining discrete ambiguity.

8.3.2. Hybrid BSS detector

The blind algorithms presented in the previous section approximate only linear spatial filters in order to separate the data streams. This reaches only a fractional amount of the performance reached by iterative detection algorithms as can be seen in Figure 8.5 for the nonblind case.

In this section we improve the detection performance by applying a cancelation scheme. This utilizes the finite symbol alphabet that was only used marginally up to now and results in a hybrid scheme that is initialized using a linear detection and iteratively improved using a symbol detection in order to obtain a totally blind scheme up to the point of the final symbol decision.[8]

We propose a system as depicted in Figure 8.6. We start with coarsely decided symbols $\hat{\mathbf{s}}$ that were obtained using a blind separation method (e.g., JADE) and

[8]This scheme can also be applied in semiblind setups using very few pilot symbols.

phase correction (8.42) described above.[9] Using this data we produce a first channel estimate $\tilde{\mathbf{H}}$. This channel estimate is used to detect the symbols once more using the MMSE-SIC as presented in Section 8.2.3. Using the output of the SIC detector for an improved channel estimation in combination with a further detection of the data will iteratively lead to better results.

The whole detection scheme remains blind, since this detection loop is blindly initialized and the SIC algorithm only decides symbol positions with quadrant ambiguities $\hat{s}_1, \ldots, \hat{s}_{N_T}$. It has to be proven that despite these ambiguities the iterations work properly. Therefore we assume that the matrix of estimated symbols $\hat{\mathbf{S}} = [\hat{\mathbf{s}}[1], \hat{\mathbf{s}}[2], \ldots, \hat{\mathbf{s}}[M]]$ achieved by the blind source separation is given by

$$\hat{\mathbf{S}} = \mathcal{Q}_{\mathcal{A}}\{\hat{\mathbf{\Psi}}\mathbf{P}\mathbf{S}\}. \tag{8.43}$$

In (8.43), $\mathbf{S} = [\mathbf{s}[1], \mathbf{s}[2] \cdots \mathbf{s}[M]]$ is the matrix of transmitted symbols, $\mathbf{P}$ is a permutation matrix, and $\hat{\mathbf{\Psi}}$ defines the diagonal matrix modeling the discrete quadrant ambiguities.

In order to use these BSS decision results $\hat{\mathbf{S}}$ for a first channel estimation we calculate

$$\tilde{\mathbf{H}} = \mathbf{R} \cdot \hat{\mathbf{S}}^{+} \tag{8.44}$$

using the matrix of the received symbols $\mathbf{R} = [\mathbf{r}[1], \mathbf{r}[2] \cdots \mathbf{r}[M]]$. After inserting (8.43) and assuming only a few decision errors, we can simplify the channel estimation [28] to

$$\tilde{\mathbf{H}} = \mathbf{H} \cdot \mathbf{P}^{H}\hat{\mathbf{\Psi}}^{H}. \tag{8.45}$$

This leads to an estimation $\tilde{\mathbf{H}}$ of the channel matrix $\mathbf{H}$ in a permuted form, where every column contains a quadrant ambiguity.

If we use the estimated channel matrix $\tilde{\mathbf{H}}$ again for the detection, we should find the data streams permuted and rotated in the same way as in (8.43). To show that this channel estimation leads to the same permutation and rotation, a simple linear detection is used:

$$\begin{aligned}\hat{\mathbf{S}} &= \mathcal{Q}_{\mathcal{A}}\{(\mathbf{H} \cdot \mathbf{P}^{H}\hat{\mathbf{\Psi}}^{H})^{+}\mathbf{R}\} = \mathcal{Q}_{\mathcal{A}}\{\hat{\mathbf{\Psi}}\mathbf{P}\mathbf{H}^{+} \cdot (\mathbf{H}\mathbf{S} + \mathbf{V})\} \\ &\approx \mathcal{Q}_{\mathcal{A}}\{\hat{\mathbf{\Psi}}\mathbf{P}\mathbf{H}^{+} \cdot \mathbf{H}\mathbf{S}\} = \mathcal{Q}_{\mathcal{A}}\{\hat{\mathbf{\Psi}}\mathbf{P}\mathbf{S}\}.\end{aligned} \tag{8.46}$$

[9] We need to start with a coarse data decision and cannot rely on the separation matrices $\mathbf{B}$ and $\mathbf{W}$ since these matrices do perform well for separation but do not include a correct amplitude estimation of the signals and therefore every cancelation scheme will fail without a first data decision.

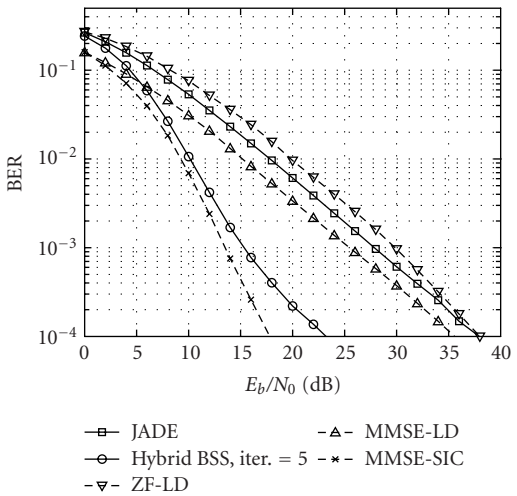

FIGURE 8.7. BER of hybrid BSS detector, $N_T = N_R = 4$, QPSK.

Therefore iterating between detection and channel estimation in a blind way leads to a stable solution of $\tilde{\mathbf{H}}$ with permutation and quadrant ambiguity.

If we apply this channel estimation in the SIC algorithm we get symbols $\hat{\mathbf{s}}$ (Figure 8.6) with the corresponding discrete quadrant ambiguities $\hat{\Psi}$, but this does not influence our further detection and cancelation process, as long as we only want to decide symbols from the alphabet $\mathcal{A}$.

To summarize, we found an iterative estimation and detection scheme that utilizes the finite symbol alphabet and remains completely blind.

Performance of the proposed iterative scheme. In order to show the feasibility of our detection approach we present some BER results of the blind source separation and the hybrid approach (Figure 8.6). As an initialization we exemplary use the output of the JADE algorithm.

Figure 8.7 depicts the results of our simulations. Beside the reference curves of the MMSE and zero-forcing linear detection the MMSE-SIC detection with ideal known channel matrix was introduced as a further reference. The performance of the blind JADE algorithm is between the ZF- and the MMSE-linear detection.

Using the proposed iterative scheme we can observe a gain of about 10 dB at a bit error rate of 10^{-3} (hybrid BSS, iterations = 5) compared to the classical source separation using the JADE algorithm only. For this improvement we need only 5 iterations of detection and channel estimation. We nearly reach the curve of the SIC algorithm with perfectly known channel matrix $\mathbf{H}$.[10] We have to emphasize that the whole detection scheme remains blind since no reference data is used in order to gain the symbol decisions.

[10]We can even decrease the gap to the detection with ideally known channel matrix if we increase the length M of the data block.

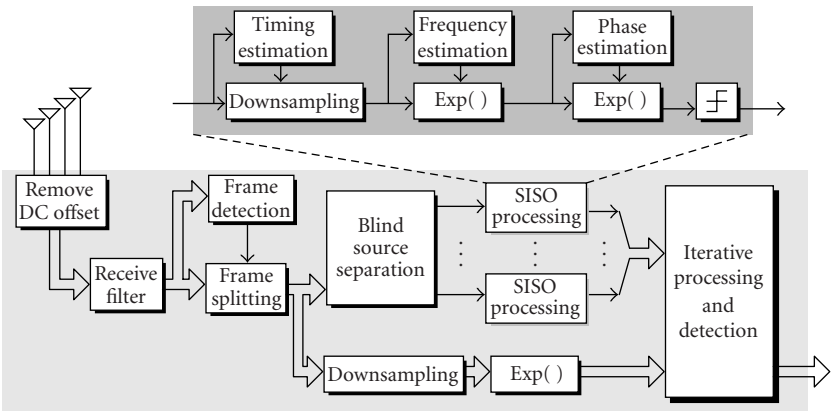

FIGURE 8.8. Receiver setup in case of hybrid blind source separation.

8.4. Experimental results—measurements

In this section some experiments of transmissions using reference-based and blind schemes are presented. As a MIMO demonstrator we used our multiple-antenna system for ISM-band transmission (MASI). This system can be applied to realize MIMO systems of up to 8 transmit and 8 receive antennas [29]. The transmission experiments are executed in real time while the processing is done offline using an interface to Matlab.

Figure 8.8 depicts the receiver setup considering exemplarily a source-separation-based transmission system. To realize transmissions, some practical problems have to be solved. First of all the DC offset caused by the direct conversion front end of the receiver has to be removed. A coarse frame detection based on a power estimation is carried out. Timing and frequency estimation have to be realized before the symbol rate processing can be accomplished.

In order to show the feasibility of the proposed approaches, the MIMO system with $N_T = 4$ antennas, and $N_R = 4$ antennas, and QPSK signals is considered. The presented measurements are carried out with a sampling frequency of $f_s = 50$ MHz. With an oversampling of $w = 8$ we can consider the transmission channel as nearly flat. The distance between transmitter and receiver was spanning two office rooms.

8.4.1. Reference-based SIC detection

For the proposed scheme we investigate two examples for reference-based transmissions. Figure 8.9 shows the eigenvalues λ_p of $\mathbf{H}^H\mathbf{H}$ ($\lambda_p = \sigma_p^2$ with σ_p denoting the singular value of $\mathbf{H}$) and the signal spaces at the slicer inputs, corresponding to Figure 8.4. Since four eigenvalues contribute to the signal transmission, the slicer input signals correspond to the modulation alphabet leading to a sufficient signal detection.

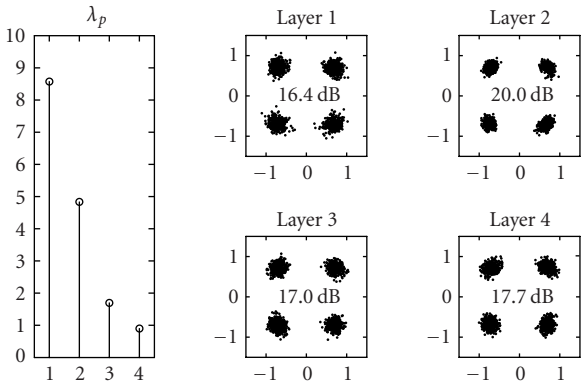

FIGURE 8.9. Eigenvalue profile and signal space diagrams for good channel condition.

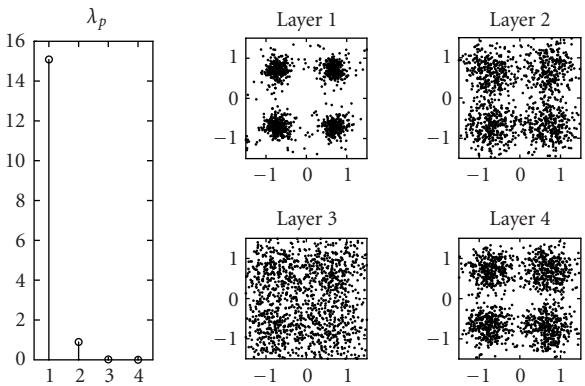

FIGURE 8.10. Eigenvalue profile and signal space diagrams for bad channel conditions.

Figure 8.10 shows a second measurement in the same office environment with slightly changed positions. In contrast to the first example, only two strong eigenvalues contribute to the transmission. The third and fourth eigenvalues are almost zero and the detection process fails.

8.4.2. Hybrid BSS detection with iterative refinement

In this section, we show the performance of the *hybrid blind source-separation-based detector* by some measurements. The setup used is depicted in Figure 8.8. To separate the independent components, the BSS algorithm is directly applied to the oversampled signal. For this step we choose the JADE [21] algorithm as a spatial separation approach. The separation leads to data streams which are processed in the classical way like in single-antenna systems. This is a considerable advantage, since well-known algorithms (e.g., for timing and for frequency synchronization) can be applied for the separated layers of MIMO systems. We synchronize to the

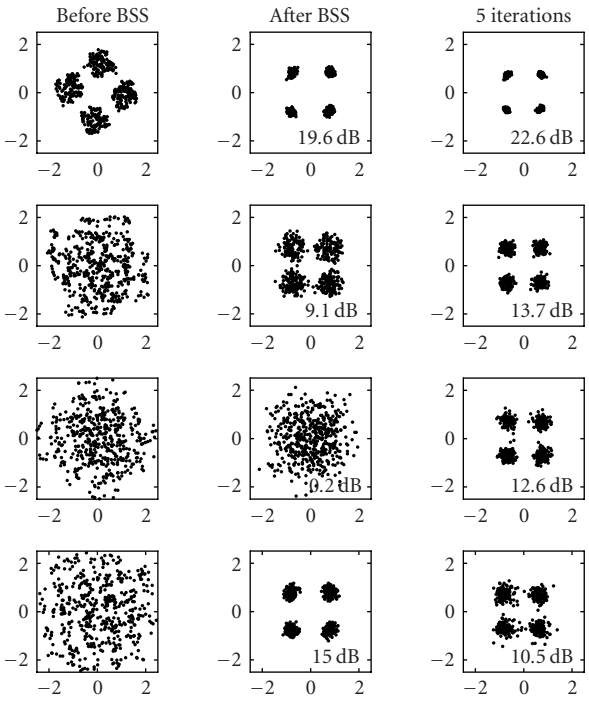

FIGURE 8.11. Signal constellations before and after blind source separation and after 5 iterations, together with blindly estimated SNR.

symbol timing using the method presented in [30]. In order to determine the carrier frequency offset we apply a non-linearity and frequency estimation.

Figure 8.11 depicts the signal constellation at symbol rate before separation, after separation, and after 5 iterations of the scheme presented in Figure 8.6. We have included estimations of the SNR of the symbol constellation before the decision devices [31]. In Figure 8.11 one of the signal constellations after BSS consists of noise only. Using the proposed iteration scheme with SIC detection and iterative channel estimation, even this constellation can be resolved to QPSK. Denote that the overall SNR has been improved.

8.5. Conclusions

Within this contribution, architectures for reference-based and blind detection of multilayer systems have been investigated. In case of known channel state information at the receiver a computational efficient detection algorithm has been proposed. Without any channel state information, we proposed a hybrid combination of blind source separation with successive interference cancelation. To ensure the feasibility of the distinct approaches, real-world transmissions have been carried out. It has been shown that the measurements correspond to the predicted

theoretical results. The feasibility of the proposed schemes have been shown in an indoor office scenario.

Abbreviations

BER	Bit error rate
BSE	Blind source extraction
BSS	Blind source separation
CSI	Channel state information
EVD	Eigenvalue decomposition
HOS	Higher-order statistics
JADE	Joint approximate diagonalization of eigenmatrices
LD	Linear detector
MASI	Multiple-antenna system for ISM-band transmission
MIMO	Multi-input multi-output
ML	Maximum likelihood
MSE	Minimum mean square error
MMSE-SIC	Minimum mean square error-successive interference cancelation
PSA	Postsorting algorithm
SIC	Successive interference cancelation
SINR	Signal-interference-and-noise ratio
SISO	Single-input single-output
SNR	Signal-to-noise ratio
SOBI	Second-order blind identification
SQRD	Sorted QR decomposition
SVD	Singular value decomposition
V-BLAST	Vertical Bell Labs Layered Space-Time
ZF	Zero forcing
ZF-SIC	Zero-forcing successive interference cancelation

Bibliography

[1] G. J. Foschini, "Layered space-time architecture for wireless communication in a fading environment when using multiple antennas," *Bell Labs. Tech. J.*, vol. 1, no. 2, pp. 41–59, 1996.

[2] P. W. Wolniansky, G. J. Foschini, G. D. Golden, and R. A. Valenzuela, "V-BLAST: an architecture for realizing very high data rates over the rich-scattering wireless channel," in *Proc. International Symposium on Signals, Systems, and Electronics (ISSSE '98)*, pp. 295–300, Pisa, Italy, September 1998.

[3] G. Strang, *Linear Algebra and Its Applications*, Harcourt Brace Jovanovich College Publishers, Orlando, Fla, USA, 3rd edition, 1988.

[4] E. Agrell, T. Eriksson, A. Vardy, and K. Zeger, "Closest point search in lattices," *IEEE Trans. Inform. Theory*, vol. 48, no. 8, pp. 2201–2214, 2002.

[5] C. Windpassinger and R. F. H. Fischer, "Low-complexity near-maximum-likelihood detection and precoding for MIMO systems using lattice reduction," in *Proc. IEEE Information Theory Workshop (ITW '03)*, pp. 345–348, Paris, France, March 2003.

[6] D. Wübben, R. Böhnke, V. Kühn, and K.-D. Kammeyer, "Near-maximum-likelihood detection of MIMO systems using MMSE-based lattice reduction," in *Proc. IEEE International Conference on Communications (ICC '04)*, Paris, France, June 2004.

[7] B. Hassibi, "An efficient square-root algorithm for BLAST," in *Proc. IEEE International Conference on Acoustics, Speech, and Signal Processing (ICASSP '00)*, vol. 2, pp. II737–II740, Istanbul, Turkey, June 2000.

[8] D. Wübben, R. Böhnke, V. Kühn, and K.-D. Kammeyer, "MMSE extension of V-BLAST based on sorted QR decomposition," in *Proc. IEEE 58th Vehicular Technology Conference (VTC '03)*, vol. 1, pp. 508–512, Orlando, Fla, USA, October 2003.

[9] A. Benjebbour, H. Murata, and S. Yoshida, "Comparison of ordered successive receivers for space-time transmission," in *Proc. IEEE VTS 54th Vehicular Technology Conference (VTC '01)*, vol. 4, pp. 2053–2057, Atlantic City, NJ, USA, October 2001.

[10] E. Bingham and A. Hyvärinen, "A fast fixed-point algorithm for independent component analysis of complex valued signals," *Int. J. Neural Syst.*, vol. 10, no. 1, pp. 1–8, 2000.

[11] D. Wübben, J. Rinas, R. Böhnke, V. Kühn, and K.-D. Kammeyer, "Efficient algorithm for detecting layered space-time codes," in *Proc. 4th International ITG Conference on Source and Channel Coding*, pp. 399–405, Berlin, Germany, January 2002.

[12] G. J. Foschini, G. D. Golden, A. Valenzuela, and P. W. Wolniansky, "Simplified processing for high spectral efficiency wireless communication employing multi-element arrays," *IEEE J. Select. Areas Commun.*, vol. 17, no. 11, pp. 1841–1852, 1999.

[13] D. W. Waters and J. R. Barry, "Noise-predictive decision feedback detection for multiple-input multiple-output channels," in *Proc. IEEE International Symposium on Advances in Wireless Communications (ISWC '02)*, Victoria, British Columbia, Canada, September 2002.

[14] D. Wübben, R. Böhnke, J. Rinas, V. Kühn, and K.-D. Kammeyer, "Efficient algorithm for decoding layered space-time codes," *IEE Electronics Letters*, vol. 37, no. 22, pp. 1348–1350, 2001.

[15] E. Biglieri, G. Taricco, and A. Tulino, "Decoding space-time codes with BLAST architectures," *IEEE Trans. Signal Processing*, vol. 50, no. 10, pp. 2547–2551, 2002.

[16] R. Böhnke, D. Wübben, V. V. Kühn, and K.-D. Kammeyer, "Reduced complexity MMSE detection for BLAST architectures," in *Proc. IEEE Global Telecommunications Conference (GLOBECOM '03)*, vol. 4, pp. 2258–2262, San Francisco, Calif, USA, December 2003.

[17] G. Ginis and J. M. Cioffi, "On the relation between V-BLAST and the GDFE," *IEEE Commun. Lett.*, vol. 5, no. 9, pp. 364–366, 2001.

[18] J.-F. Cardoso, "The three easy routes to independent component analysis; contrasts and geometry," in *Proc. Idaho Counseling Association (ICA '01)*, San Diego, Calif, USA, December 2001.

[19] A. Belouchrani, K. Abed-Meraim, J.-F. Cardoso, and E. Moulines, "A blind source separation technique using second-order statistics," *IEEE Trans. Signal Processing*, vol. 45, no. 2, pp. 434–444, 1997.

[20] A. Cichocki and S. Amari, *Adaptive Blind Signal and Image Processing*, Wiley, New York, NY, USA, 2002.

[21] J.-F. Cardoso and A. Souloumiac, "Blind beamforming for non-Gaussian signals," *IEE Proceedings F, Radar and Signal Processing*, vol. 140, no. 6, pp. 362–370, 1993.

[22] S. Haykin, Ed., *Unsupervised Adaptive Filtering, Volume 1, Blind Source Separation*, Adaptive and Learning Systems for Signal Processing, Communications and Control. Wiley Interscience, New York, NY, USA, 2000.

[23] A. Hyvärinen, J. Karhunen, and E. Oja, *Independent Component Analysis*, Wiley, New York, 2001.

[24] F. Herrmann and A. K. Nandi, "Blind separation of linear instantaneous mixtures using closed-form estimators," *Signal Processing*, vol. 81, no. 7, pp. 1537–1556, 2001.

[25] A. Stuart and K. Ord, *Kendall's Advanced Theory of Statistics—Volume I: Distribution Theory*, Wiley, New York, NY, USA, 6th edition, 1994.

[26] M. Feng and K.-D. Kammeyer, "Blind source separation for communication signals using antenna arrays," in *Proc. IEEE International Conference on Personal Wireless Communications (ICUPC '98)*, vol. 1, pp. 665–669, Florence, Italy, October 1998.

[27] A. Hyvärinen and E. Oja, "A fast fixed-point algorithm for independent component analysis," *Neural Computation*, vol. 9, no. 7, pp. 1483–1492, 1997.

[28] J. Rinas and K.-D. Kammeyer, "Comparison of blind source separation methods based on iterative algorithms," in *Proc. 5th International ITG Conference on Source and Channel Coding (SCC '04)*, Erlangen, Germany, January 2004.

[29] J. Rinas, R. Seeger, L. Brötje, S. Vogeler, T. Haase, and K.-D. Kammeyer, "A multiple antenna system for ISM-band transmission," *EURASIP J. Appl. Signal Process.*, vol. 2004, no. 9, pp. 1407–1419, 2004.
[30] S. J. Lee, "A new non-data-aided feedforward symbol timing estimator using two samples per symbol," *IEEE Commun. Lett.*, vol. 6, no. 5, pp. 205–207, 2002.
[31] R. Matzner, "An SNR estimation algorithm for complex baseband signals using higher order statistics," *Facta Universitatis: Electronics and Energetics*, vol. 6, no. 1, pp. 41–52, 1993.
[32] J. Rinas and K.-D. Kammeyer, "MIMO measurements of communication signals and application of blind source separation," in *Proc. 3rd IEEE International Symposium on Signal Processing and Information Technology (ISSPIT '03)*, pp. 94–97, Darmstadt, Germany, December 2003.

Karl-Dirk Kammeyer: Department of Communications Engineering, Universität Bremen, P.O. Box 33 04 40, 28334 Bremen, Germany
Email: kammeyer@ant.uni-breman.de

Jürgen Rinas: Department of Communications Engineering, Universität Bremen, P.O. Box 33 04 40, 28334 Bremen, Germany
Email: rinas@ant.uni-bremen.de

Dirk Wübben: Department of Communications Engineering, Universität Bremen, P.O. Box 33 04 40, 28334 Bremen, Germany
Email: wuebben@ant.uni-bremen.de